



Modeling Texture Evolution in Metals with CA Model

dr inż. Bartosz Sułkowski

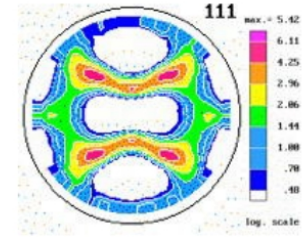
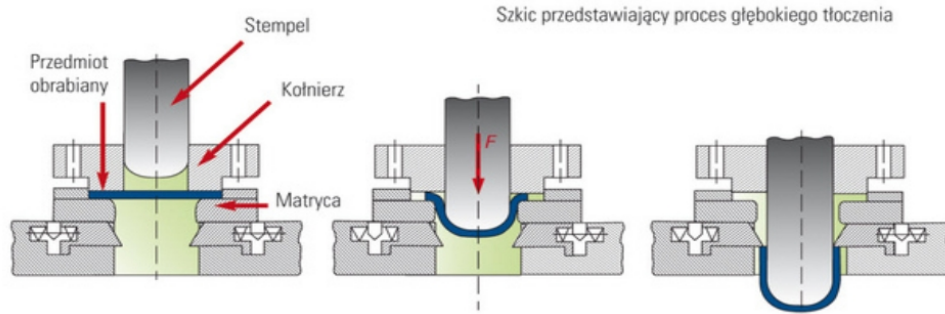
*Katedra Nauki o Materiałach i Inżynierii Metali Nieżelaznych
Wydział Metali Nieżelaznych
Akademia Górniczo-Hutnicza im. Stanisława Staszica w Krakowie*

Akademickie Centrum Komputerowe Cyfronet AGH

Motivation

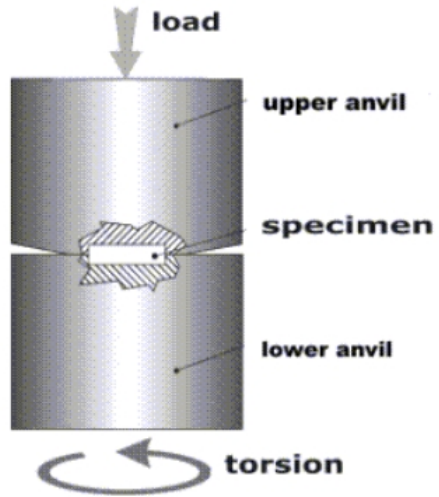
- Increasing demand for new emerging alloys e.g: automotive and transport industry,
- New applications: **hydrogen storage, biodegradable materials**
- Anisotropy of properties
- The plastic deformation of some important alloys is rather problematic due to the strong anisotropy of hexagonal structure – formation of strong basal texture during e.g. rolling
- The ductility of the alloys can be enhanced by means of weakening texture in many different ways:
 - changing of the rolling direction
 - introducing shear component of deformation e.g. in differential speed rolling processing (DSR)
 - dynamic recrystallization (DRX)
 - DRX + massive twinning during rolling at very high strain rates ($\geq 10^1 \text{ s}^{-1}$)

Anisotropy in metals

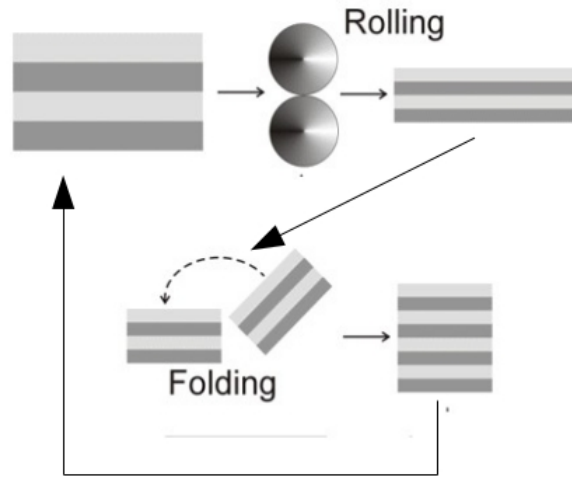


Severe plastic deformation methods

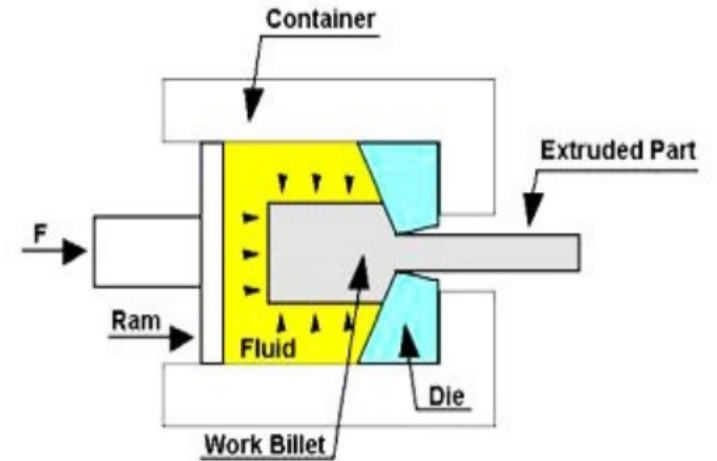
High Pressure Torsion (HPT)



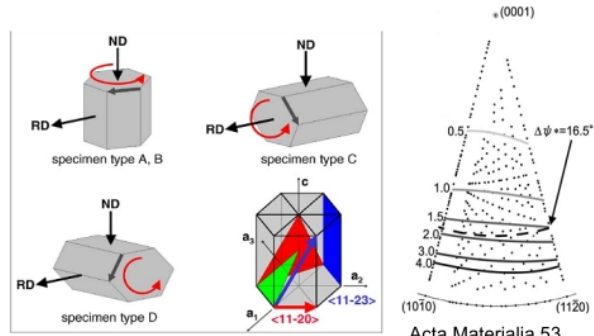
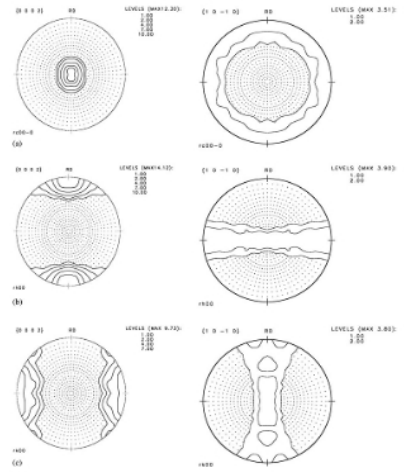
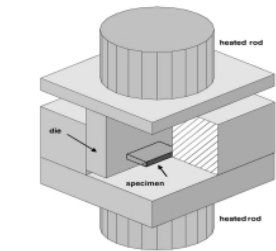
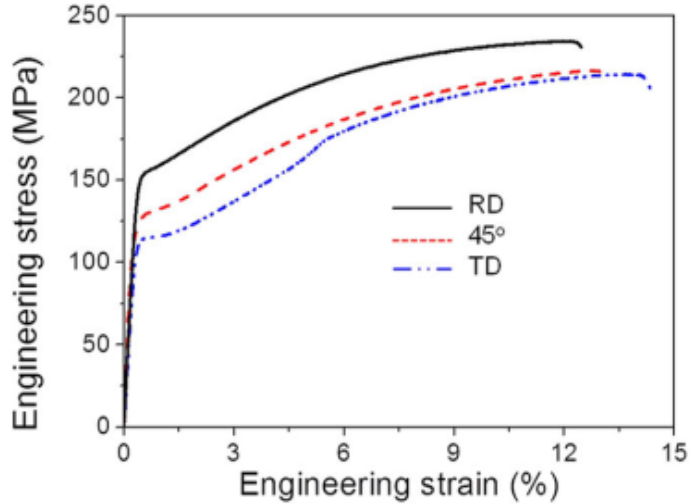
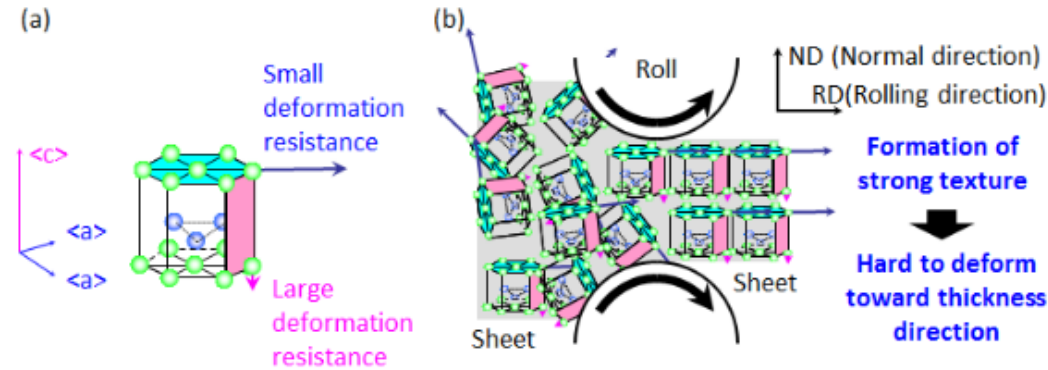
Cold Rolling and Folding (CR&F)



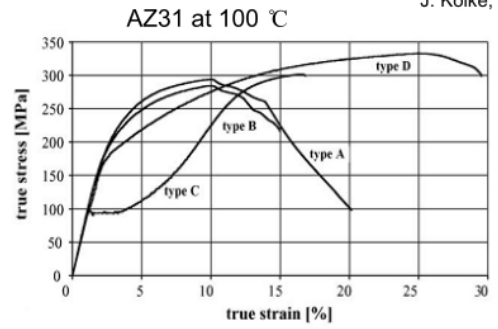
Hydrostatic Extrusion (HE)



Mechanical anisotropy of HCP metals

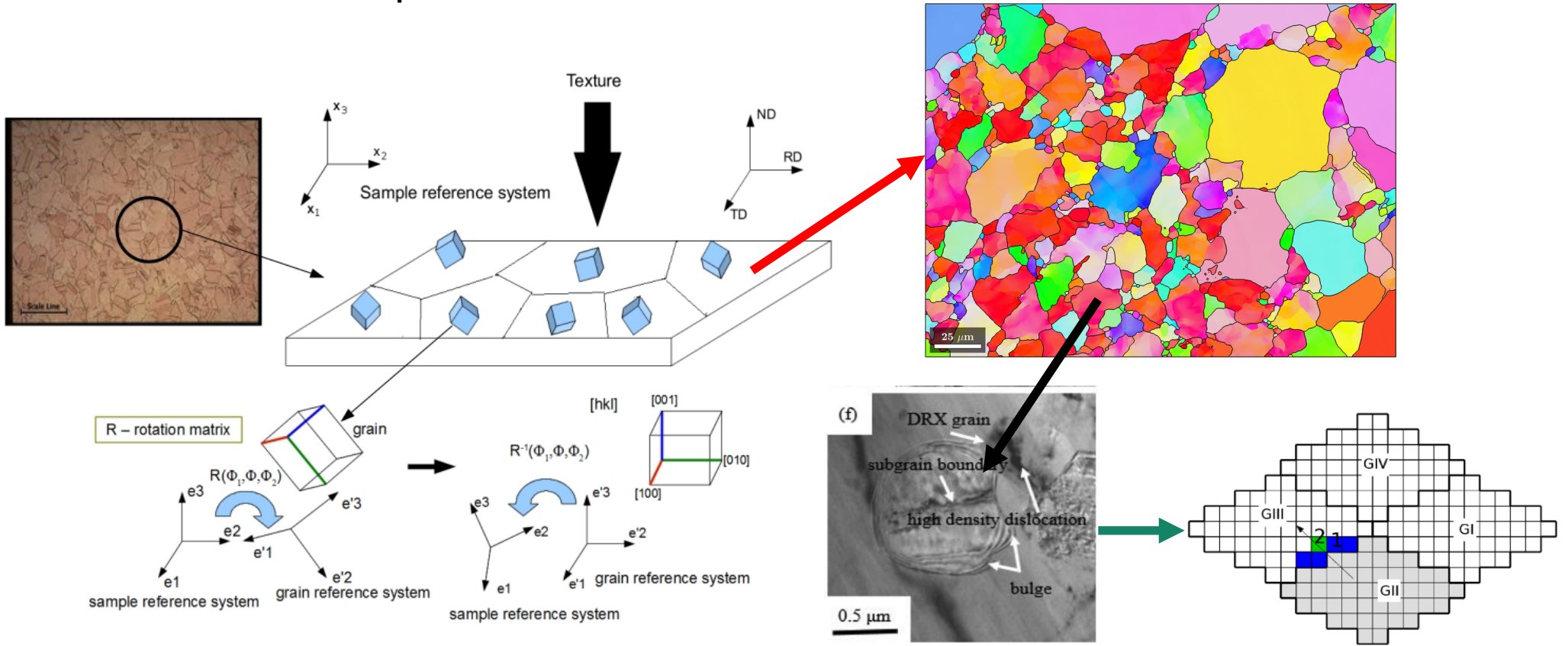


Acta Materialia 53 (2005) 1963–1972
J. Koike, R. Ohyama



Materials Science and Engineering A 395 (2005) 338–34
R. Gehrman, M.M. Frommert, G. Gottstein

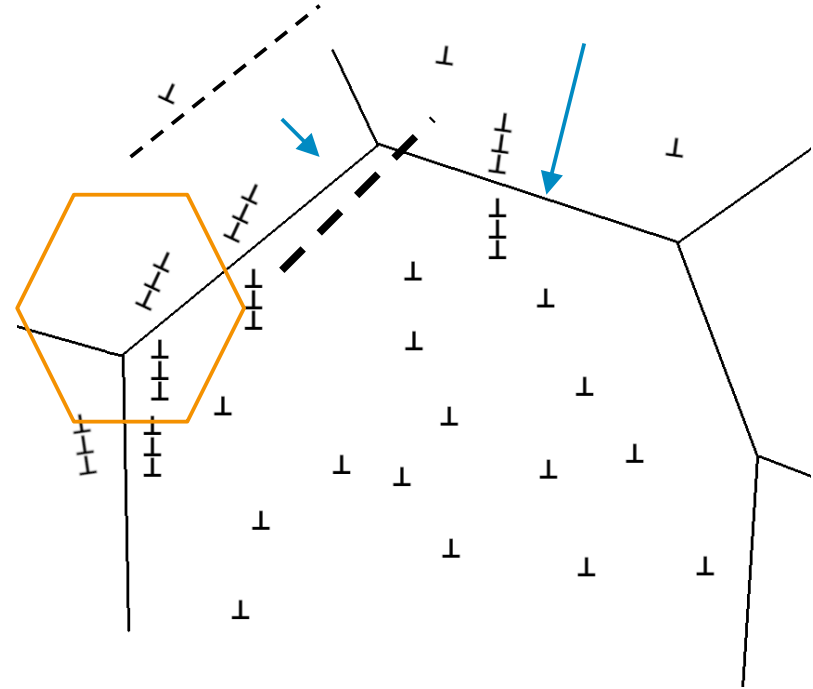
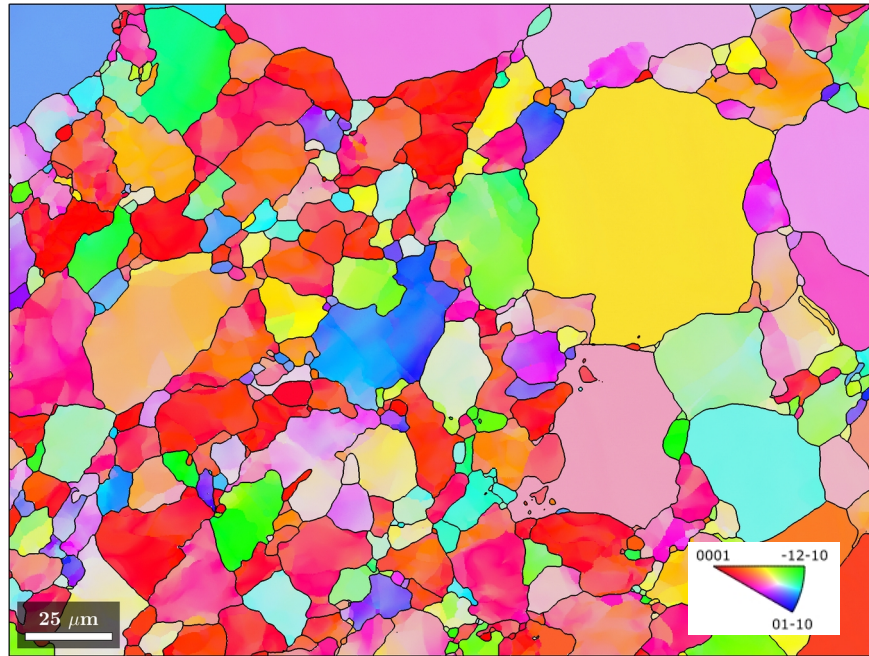
Substructure in hcp metals



$d \approx 20-30 \mu\text{m}$ \longrightarrow in 1 cm^3 is about 10^7 grains

Meijuan Hao et al.,
 Texture evolution induced by twinning and dynamic recrystallization in dilute Mg-1Sn-1Zn-1Al alloy during hot compression,
 10.1016/j.jma.2019.10.002, Journal of Magnesium and Alloys, 2020

Dislocation structure in the grains

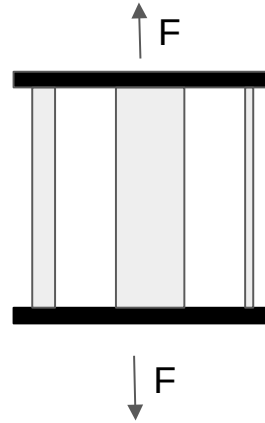


Models for texture evolution in deformed metals

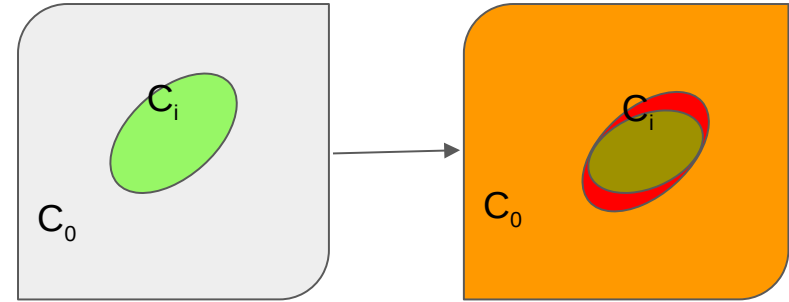
Model Sachsa



Model Taylora



Model vpssc



$$\dot{\gamma}_s = \dot{\gamma}_0 \left(\left| \frac{\tau_c^s}{\tau_0^s} \right| \right)^{\frac{1}{m}} \text{sign}(\tau_c^s)$$

$$\tau_c^s = \tau_0^s + (\tau_1^s + \theta_1^s) \left(1 - \exp\left(\frac{-\theta_0^s}{(\tau_1^s)} \right) \right)$$

- P. Van Houtte, A Comprehensive Mathematical Formulation of an Extended Taylor-Bishop-Hill Model Featuring Relaxed Constraints, the Renouard-Wintenberger Theory and a Strain Rate Sensitivity Model, Textures and Microstructures, 8-9 (1988), 313-350
- P. Van Houtte, S. Li, M. Seefeldt, L. Delannay, Deformation texture prediction: from the Taylor model to the advanced Lamel model, International Journal of Plasticity 21 (2005), 589-624
- S. Graff, Micromechanical Modeling of the Deformation of HCP Metals, GKSS-Forschungszentrum Geesthacht GmbH, Geesthacht, (2008)
- H.R. Piehler, Crystal-Plasticity Fundamentals, ASM Handbook Volume 22A: Fundamentals of Modeling for Metals Processing (2009)
- H. Wang, P.D. Wu, J. Wang, C.N. Tomé, A crystal plasticity model for hexagonal close packed (HCP) crystals including twinning and de-twinning mechanisms, International Journal of Plasticity 49 (2013), 36-52

Model for texture evolution in hot deformed metals

1	7	7	5	5	6
1	1	5	5	5	5
1	1	5	5	5	5
1	2	2	2	5	4
3	2	2	2	4	4
3	3	2	2	4	4

- D. Raabe, Introduction of a scalable three-dimensional cellular automaton, with a probabilistic switching rule for the discrete mesoscale simulation of recrystallization phenomena, Philosophical Magazine A, 79 (1999), 2339-2358
- D. Raabe, L. Hantcherli, 2D cellular automaton simulation of the recrystallization texture of an IF sheet steel under consideration of Zener pinning, Computational Materials Science 34 (2005), 299-313
- L. Wang, G. Fanga, L. Qian, Modeling of dynamic recrystallization of magnesium alloy using cellular automata considering initial topology of grains, Materials Science and Engineering A 711 (2018), 268-283

$$\dot{x} = n\eta p = n\eta_0 \exp\left(\frac{-Q_{GB}}{k_B T}\right) p$$

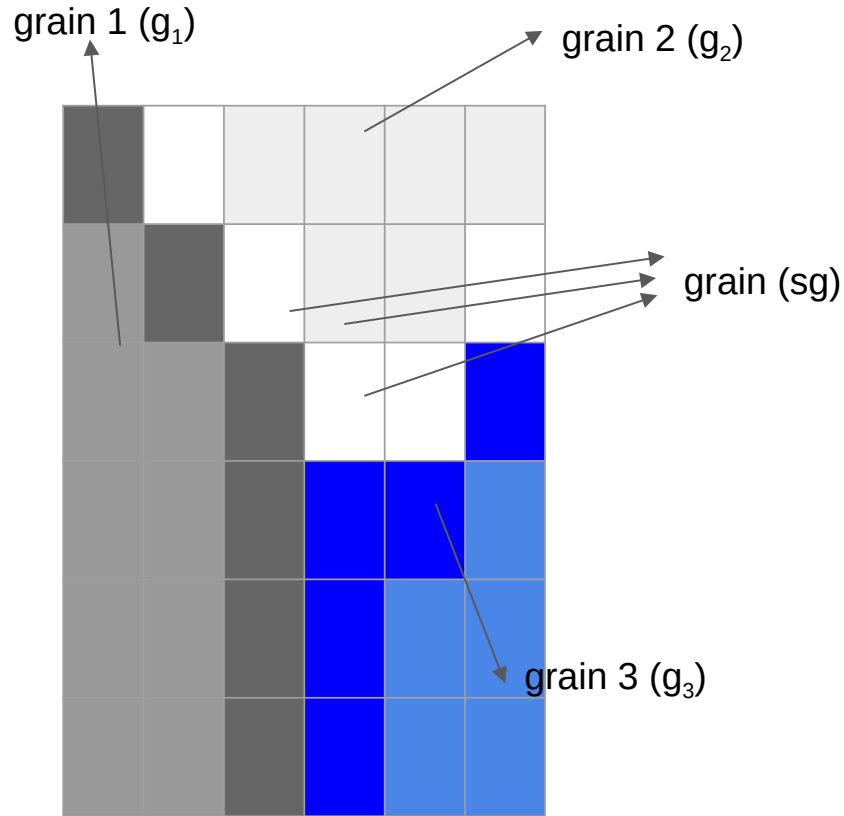
- \dot{x} – prędkość przemieszczania się granicy ziarna,
 n – normalna do płaszczyzny granicy ziarna,
 η, η_0 – parametry opisujące ruchliwość granicy ziarna,
 Q_{GB} – energia aktywacji przemieszczania się granicy ziarna,
 k_B – stała Boltzmanna,
 T – temperatura bezwzględna,
 p – parametr opisujący sumaryczne naprężenie pędne działające na granicę ziarna.

$$w^{ij} = \zeta \left(\frac{\eta_0^{ij} p^{ij}}{\eta_0^{\max} p^{\max}} \right) \exp\left(\frac{Q^{ij}}{k_B T}\right)$$

- w^{ij} – prawdopodobieństwo zmiany stanu komórki c_i na stan komórki c_j ,
 ζ – maksymalna dozwolona wariancja,
 η_0^{ij} – mobilność granicy ziarna pomiędzy komórkami c_i i c_j ,
 p^{ij} – naprężenia działające na granicę ziarna między komórkami c_i i c_j ,
 η_0^{\max} – maksymalna mobilność granicy ziarna,
 p^{\max} – maksymalne naprężenie działające na granicę ziarna,
 Q^{ij} – energia aktywacji przemieszczania się granicy ziarna pomiędzy komórkami c_i i c_j .

Description of the new *vpsc*+CA

B. Sulkowski, R. Chulist, Modeling of dynamic recrystallization texture in hot extruded Mg, Materials Characterization 201 (2023) 112968



$$1. \quad \forall g \forall s : \dot{\gamma}_s = \dot{\gamma}_0 \left(\left| \frac{\tau_c^s}{\tau_0^s} \right| \right)^{\frac{1}{m}} \text{sign}(\tau_c^s)$$

$$\tau_c^s = \tau_0^s + (\tau_1^s + \theta_1^s) \left(1 - \exp\left(\frac{-\theta_0^s}{\tau_1^s}\right) \right)$$

$$\forall g : \frac{d\rho_\epsilon}{d\epsilon} = K_1 \sqrt{\bar{\rho}} - K_2 \rho$$

$$\dot{\omega}_{ij} = \sum_{s=1}^n \frac{1}{2} (m_{ij}^s - m_{ji}^s) \dot{\gamma}^s$$

$$2. \quad \forall sg : \bar{\rho}_{GNDS} = \frac{2\theta_{nm}}{n\lambda|b_d|}, n \neq m$$

$$\bar{\rho} = \rho_\epsilon + \bar{\rho}_{GNDS}$$

grain boundaries movement

$$w^{nm} = \sigma \left(\frac{m_0^{nm} p^{nm}}{m_0^{max} p^{max}} \right) \exp \frac{-Q_{nm}^{local} + Q_{nm}^{min}}{k_B T}$$

akceptuj ješli $r \leq w^{nm}$

odrzuć ješli $r > w^{nm}$

nucleation

$$\rho_c = \left(\frac{20\gamma\dot{\epsilon}}{3b|M|\tau^2} \right)^{1/3}$$

Experiments and simulations

Mg, AZ31, AM50, AZ61 →

↓
rolling, extrusion
180°C, 280°C, 380°C

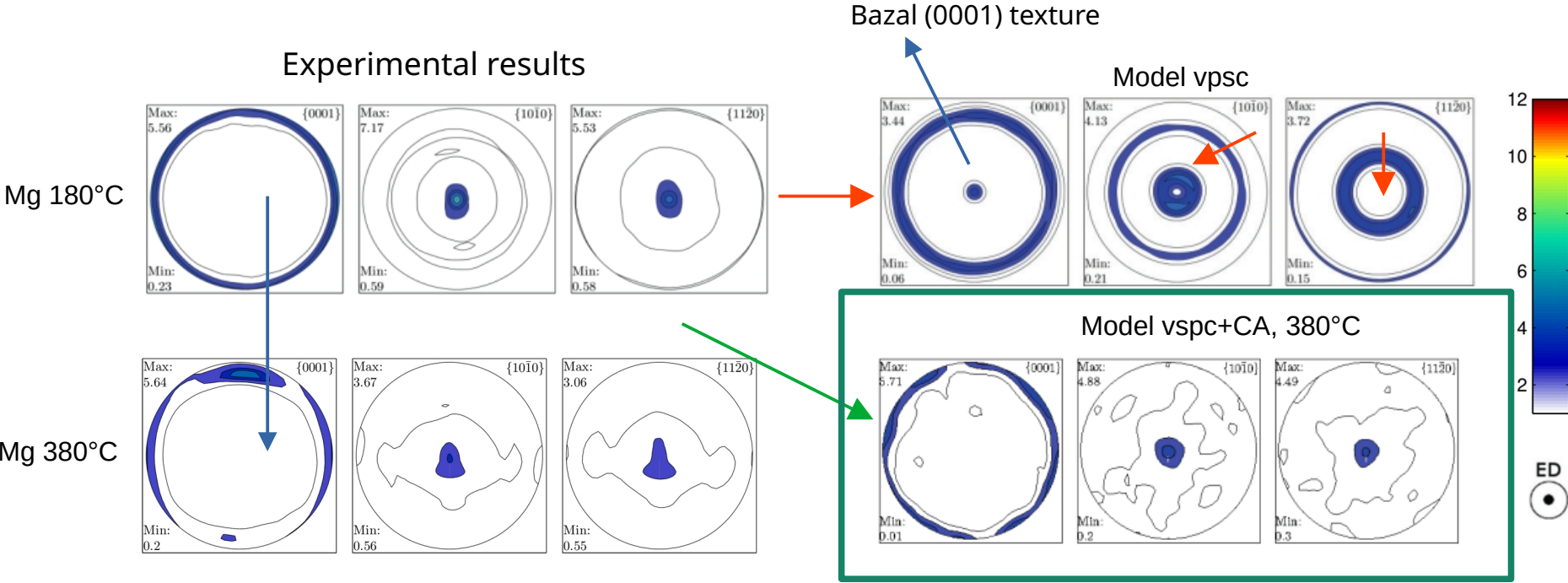
↓
structural investigations, EBSD, texture

↓
simulations
• vpsc
• vpsc+CA

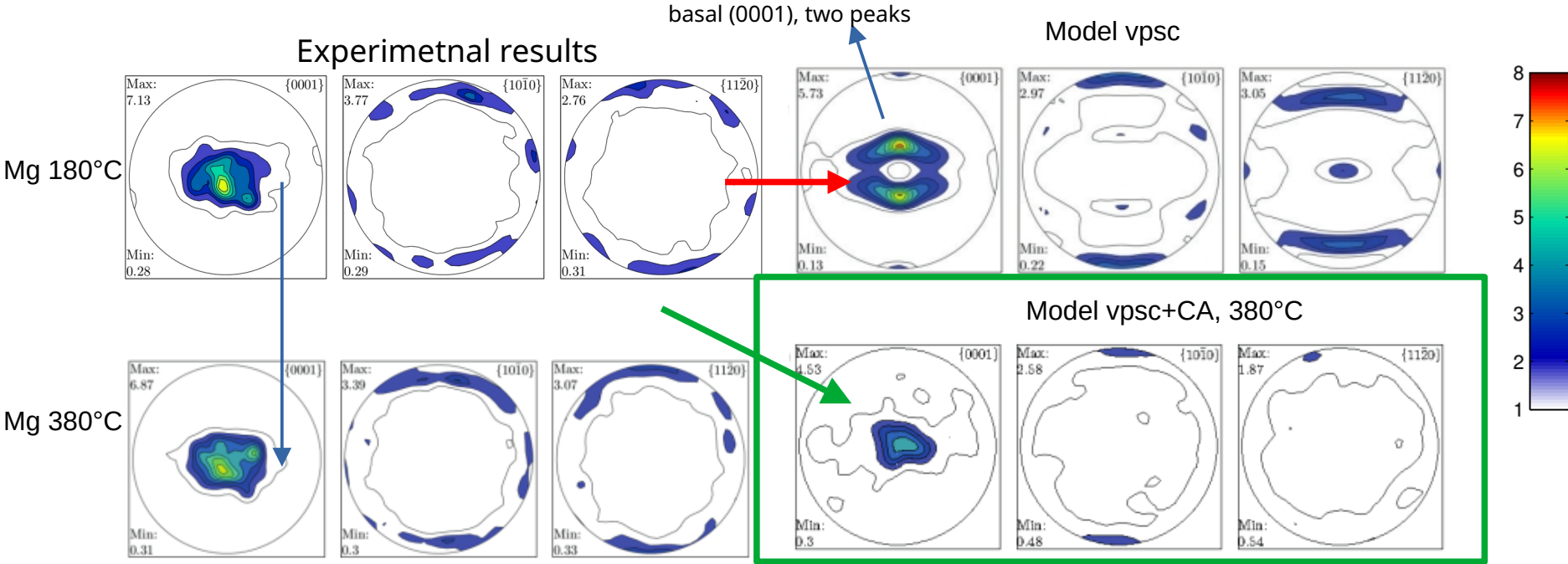
Stop (ASTM)	PN-EN 1753:2001	Al (% wag.)	Zn (% wag.)	Mn (% wag.)	Mg (% wag.)
Mg	EN-MCMg99,8	-	-	-	99,8
AZ31	EN-MCMgAl3Zn1	2,5-3,5	0,6-1,4	-	reszta
AM50	EN-MCMgAl1Mn0	4,4-5,4	0,22	0,26-0,6	reszta
AZ61	EN-MCMgAl6Zn1	5,8-7,2	0,4-1,5	-	reszta

- Number of grains $10^3 - 10^5$
- Number of subgrains for each grain 36 - 64
- MPI libraries
- Ares Supecomputer
- 1 node x 1 cpu - 4 nodes x 48 cpus

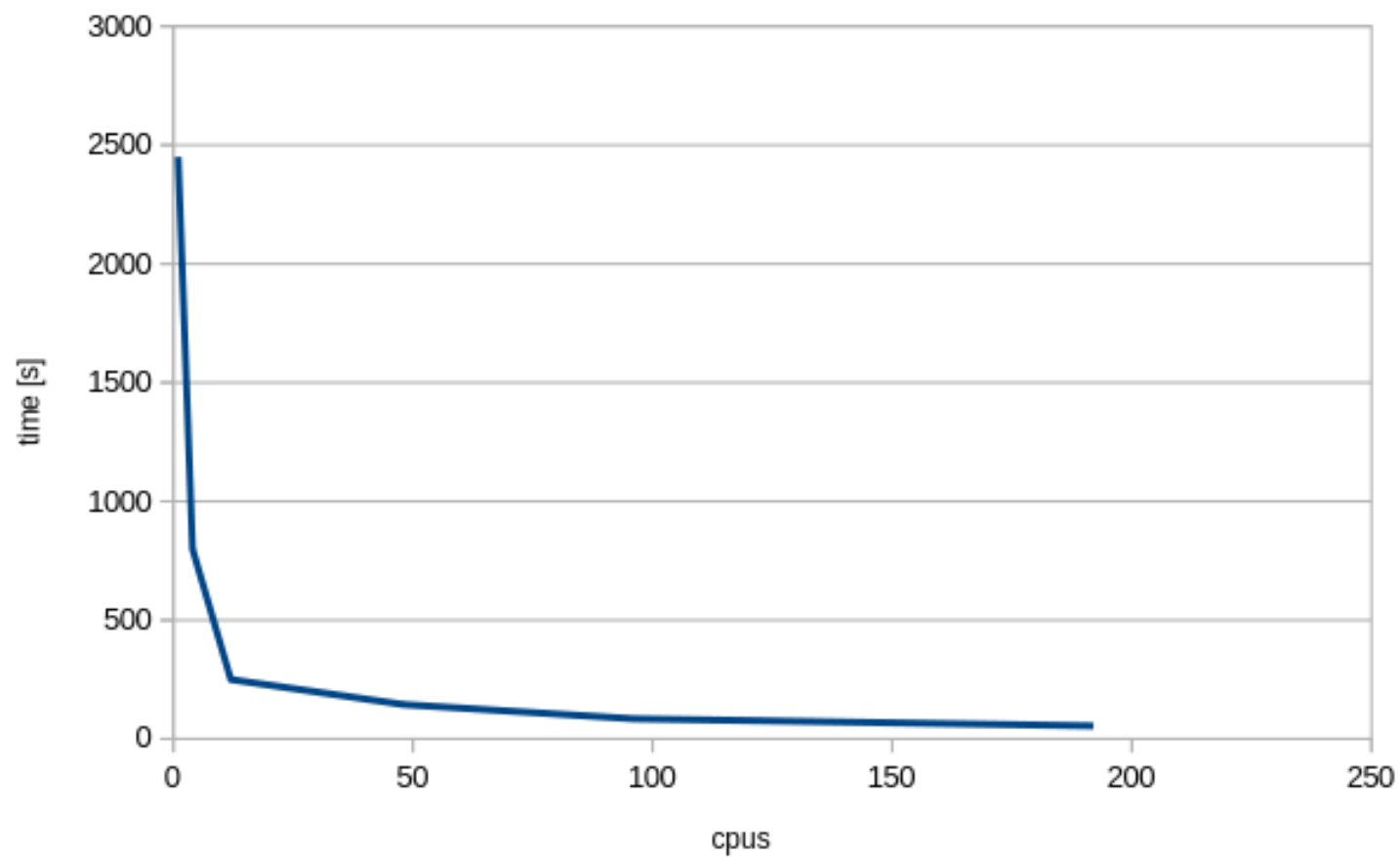
Results for extrusion



Results for rolling



Calculation time



Summary

- Main texture component during rolling is basal
- Main texture component during extrusion is $\{10-10\}$ fibre and $\{11-20\}$ fibre
- During hot deformation texture is weakened
- VSCP model can't predict hot deformed texture
- VSCP+CA predictions of texture are comparable with experiments
- Due to the complexity of vpsc+CA model parallel calculations on supercomputer have to be performed

Thank you for your attention